European Journal of Medicinal Chemistry 45 (2010) 5353–5361

Contents lists available at ScienceDirect

European Journal of Medicinal Chemistry

journal homepage: http://www.elsevier.com/locate/ejmech

Original article

Crystal structures, DNA-binding and cytotoxic activities studies of Cu(II) complexes with 2-oxo-quinoline-3-carbaldehyde Schiff-bases

Zeng-Chen Liu [a], Bao-Dui Wang [a], Bo Li [b], Qin Wang [b], Zheng-Yin Yang [a,*], Tian-Rong Li [a], Yong Li [a]

[a] College of Chemistry and Chemical Engineering, State Key Laboratory of Applied Organic Chemistry, Lanzhou University, Lanzhou 730000, PR China
[b] College of Life Science, Lanzhou University, Lanzhou 730000, PR China

ARTICLE INFO

Article history:
Received 27 May 2010
Received in revised form
26 August 2010
Accepted 26 August 2010
Available online 15 September 2010

Keywords:
2-Oxo-quinoline-3-carbaldehyde Schiff-base
Crystal structure
DNA-binding
Cytotoxic activity

ABSTRACT

Three novel 2-oxo-quinoline-3-carbaldehyde Schiff-bases and their Cu(II) complexes were synthesized. The molecular structures of Cu(II) complexes were determined by X-ray crystal diffraction. The DNA-binding modes of the complexes were also investigated by UV–vis absorption spectrum, fluorescence spectrum, viscosity measurement and EB–DNA displacement experiment. The experimental evidences indicated that the ligands and Cu(II) complexes could interact with CT-DNA (calf-thymus DNA) through intercalation, respectively. Comparative cytotoxic activities of ligands and Cu(II) complexes were also determined by MTT [3-(4,5-dimethyl-2-thiazoyl)-2,5-diphenyl-2H-tetrazolium bromide] and SRB (sulforhodamine B) methods. The results showed that the three Cu(II) complexes exhibited more effective cytotoxic activity against HL60 cells and HeLa cells than corresponding ligands. Also, CuL^3 showed higher cytotoxic activity than CuL^1 and CuL^2.

1. Introduction

There has been an increasing focus on the binding study of small molecules to DNA during the last decades, since deoxyribonucleic acid (DNA) is an important genetic substance in organisms [1–3]. And errors in gene expression can often cause diseases and play a secondary role in the outcome and severity of human diseases [4]. So a more complete understanding of DNA–drug binding is valuable in the rational design of DNA structural probe, DNA footprinting, sequence-specific cleaving agents and potential anti-cancer drugs [5,6].

In order to develop new drugs which specifically target DNA, it is necessary to understand the different binding modes which a small molecule is capable of undergoing. The recognition modes for the noncovalent binding of small molecules to DNA are intercalative binding, groove binding and external electrostatic binding [7,8]. Among these interactions, intercalation and groove binding are the most important DNA-binding modes as they invariably lead to cellular degradation. Additionally, the metal ion type and different functional groups of ligands, which are responsible for the geometry of complexes, also affect the affinity of metal complexes to DNA.

In addition, as small molecules, a great many Schiff-base complexes with transition metals have provoked wide interests because of their diverse biological and pharmaceutical activities [9,10]. In the previous literature, a number of Cu(II) complexes with biological activities such as antibacterial and anti-cancer properties have been also reported [11,12]. So the investigation on the interaction of the Schiff-base transition metal complexes with DNA has a great significance for disease defense, new medicine design and filtration and clinical application of drugs. Quinoline and its derivates, naturally occurring antibiotic, are one of the most widely utilized as antibacterial and antimalarial drugs [13–15]. Also, 2-oxo-quinoline appears frequently in the structure of various natural compounds that have biological activities [16,17]. Simultaneously, our previous work showed some Cu(II) Schiff-bases complexes derived from 2-oxo-quinoline-carbaldehyde can bind to DNA by intercalation [18]. With the increasing interest in the interaction of transition metal complexes with DNA, in this paper, three novel Schiff-base ligands derived from 2-oxo-quinoline-3-carbaldehyde and benzoyl (2-hydroxybenzoyl and 3,4-dimethyl pyrryl-2-carboxylic acid) hydrazine are designed and synthesized, moreover, their Cu(II) complexes are also characterized by X-ray crystal diffraction. And the binding modes for the interaction of the three Cu(II) complexes with CT-DNA are investigated by electronic absorption spectroscopy, fluorescence spectroscopy and viscosity measurement. The experimental results indicate that the three Cu(II) complexes can bind to DNA through intercalative binding modes. On the other hand,

* Corresponding author. Tel.: +86 931 891 3515; fax: +86 931 891 2582.
E-mail address: yangzy@lzu.edu.cn (Z.-Y. Yang).

0223-5234/$ – see front matter © 2010 Elsevier Masson SAS. All rights reserved.
doi:10.1016/j.ejmech.2010.08.060

cytotoxic activities against HeLa cell and HL60 cell were also investigated in our work. As previous reports demonstrated that several organic-copper complexes could inhibit some tumor cell growth in vitro and in human tumor cell cultures [19–21]. So there is a need to test the cytotoxic activities of the compounds. According to the experiments, it has been found that the cytotoxic activities of Cu(II) complexes are higher than that of ligands, moreover, compared with CuL^1 and CuL^2, CuL^3 exhibited more potent cytotoxic effect against the two cell lines. The results should be valuable in designing novel agents for targeting nucleic acids as well as setting the stage for the synthesis of chemical anticarcinogenic drugs.

2. Chemistry

As shown in Scheme 1, 2-oxo-quinoline-3-carbaldehyde **5** was prepared according to the literature [22]. And that the compound was characterized by NMR. 3,4-Dimethyl-2-ethoxycarbonyl-pyrrole **1** was synthesized by the reported papers [23,24]. The compositions of Cu(II) complexes were confirmed by X-ray single crystal diffraction. The three Cu(II) complexes were found to possess five coordinative square-pyramidal configuration. DNA-binding study and cytotoxic experiments were also carried out to evaluate the binding modes and potential anti-cancer activities.

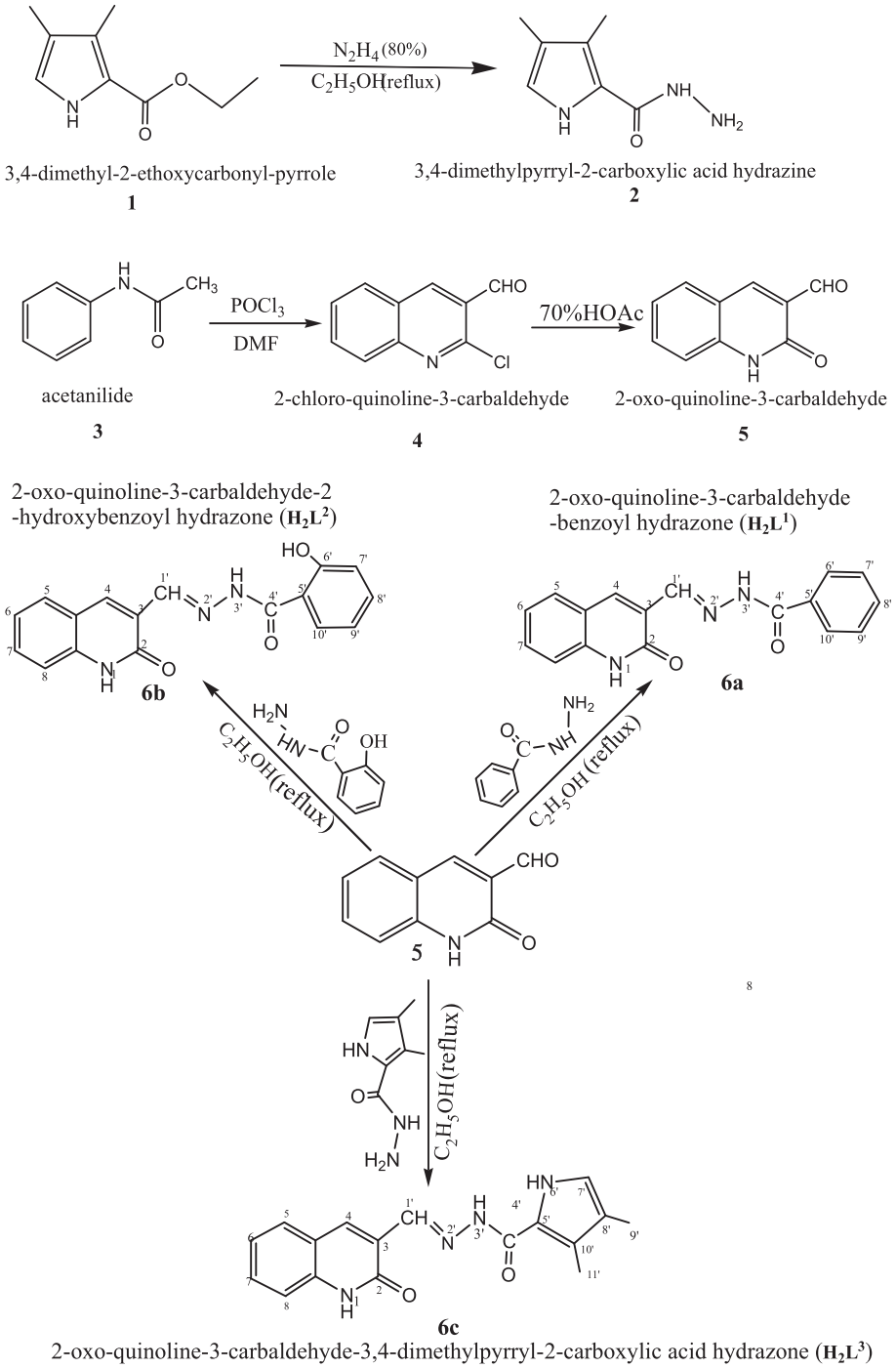

Scheme 1. The synthesis line of ligands (2-oxo-quinoline-3-carbaldehyde-benzoyl hydrazone **6a**, 2-oxo-quinoline-3-carbaldehyde-2-hydroxybenzoyl hydrazone **6b**, 2-oxo-quinoline-3-carbaldehyde-3,4-dimethylpyrryl-2-carboxylic acid hydrazone **6c**).

The results revealed that the Cu(II) complexes exhibited stronger affinity with CT-DNA.

2.1. X-ray crystallography

A green crystal of Cu(II) complex of H_2L^1 (0.35 × 0.33 × 0.29 mm) was measured on a Bruker APEX-II CCD diffractometer with graphite monochromatic Mokα radiation (λ = 0.71073 Å) at 296(2) K. The crystallographic data are given in Table 1. The intensity data were collected by the ω scan mode within $1.56° < \theta < 25.50°$ for *hkl* ($-8 \le h \le 8$, $-20 \le k \le 14$, $-24 \le l \le 25$) in the monoclinic. The positions and anisotropic thermal parameters of all non-hydrogen atoms were refined on F^2 by full-matrix least-squares techniques with the SHELX-97 program package (G. M. Sheldrick, Bruker AXS, Madison, WI, 2008). Absorption correction was employed using Semi-empirical methods from equivalents.

A green crystal of Cu(II) complex of H_2L^2 (0.35 × 0.33 × 0.27 mm) was measured on a Bruker APEX-II CCD diffractometer with graphite monochromatic Mokα radiation (λ = 0.71073 Å) at 296(2) K. The crystallographic data are given in Table 1. The intensity data were collected by the ω scan mode within $2.74° < \theta < 27.27°$ for *hkl* ($-9 \le h \le 9$, $-11 \le k \le 12$, $-15 \le l \le 18$) in the Triclinic. The positions and anisotropic thermal parameters of all non-hydrogen atoms were refined on F^2 by full-matrix least-squares techniques with the SHELX-97 program package (G. M. Sheldrick, Bruker AXS, Madison, WI, 2008). Absorption correction was employed using Semi-empirical methods from equivalents.

A brown crystal of Cu(II) complex of H_2L^3 (0.25 × 0.20 × 0.18 mm) was measured on a Bruker APEX-II CCD diffractometer with graphite monochromatic Mokα radiation (λ = 0.71073 Å) at 296(2) K. The crystallographic data are given in Table 1. The intensity data were collected by the ω scan mode within $2.22° < \theta < 25.17°$ for *hkl* ($-10 \le h \le 10$, $-11 \le k \le 13$, $-18 \le l \le 15$) in the Triclinic. The positions and anisotropic thermal parameters of all non-hydrogen atoms were refined on F^2 by full-matrix least-squares techniques with the SHELX-97 program package (G. M. Sheldrick, Bruker AXS, Madison, WI, 2008). Absorption correction was employed using Semi-empirical methods from equivalents.

Table 1
Crystal data and structure refinement of the Cu(II) complex.

	CuL^1	CuL^2	CuL^3
Formula	$C_{21}H_{29}Cu_2N_4O_9$	$C_{19}H_{19}CuN_5O_{11}$	$C_{19}H_{24}CuN_5O_8$
FW	545.02	556.93	513.97
Crystal colour	Green	Green	Brown
Crystal size (mm)	0.35 × 0.33 × 0.29	0.35 × 0.33 × 0.27	0.25 × 0.20 × 0.18
Crystal system	Monoclinic	Triclinic	Triclinic
Space group	*P*21/*c*	*P*-1	*P*-1
a (Å)	7.1988(3)	8.0506(7)	8.433(3)
b (Å)	17.4054(6)	10.4305(9)	10.339(4)
c (Å)	20.7016(6)	15.2937(13)	14.451(7)
α (°)	90.00	76.351(4)	109.571(5)
β (°)	108.271(2)	77.907(4)	92.259(8)
γ (°)	90.00	68.184(4)	107.360(6)
V (Å^3)	2463.10(15)	1147.99(17)	1119.4(8)
Z	4	2	2
D_{calc} (g/cm^3)	1.470	1.611	1.525
Abs coeff (mm^{-1})	0.944	1.022	1.031
F(000)	1136	570	532
$\theta_{min\ and\ max}$ (deg)	1.56–25.50	2.74–27.27	2.22–25.17
Reflections collected	3757/4579	3688/4438	3708/4747
Unique	[*R*(int) = 0.0331]	[*R*(int) = 0.0146]	[*R*(int) = 0.0166]
Final *R* indices	*R*1 = 0.0387	*R*1 = 0.0477	*R*1 = 0.0418
[*I* > 2sigma(*I*)]	*wR*2 = 0.1233	*wR*2 = 0.0977	*wR*2 = 0.1056
R indices	*R*1 = 0.0488,	*R*1 = 0.0367,	*R*1 = 0.0575,
(all data)	*wR*2 = 0.1321	*wR*2 = 0.0932	*wR*2 = 0.1166

2.2. Cytotoxicity assay

Tumor cell lines used in this work were grown in RPMI-1640 medium supplemented with 10% (vol/vol) calf serum 2 mmol^{-1} glutamine, 100 U mL^{-1} penicillin (U = 1 unit of activity), and 100 μg mL^{-1} streptomycin (GIB-CO, Grand Island, NY) at 310 K under 5% CO_2. Cells in 100 μL culture medium were seeded into 96-well plates (Falcon, CA), then treated with varied concentration (10, 20, 40, 80 and 160 μM) of the compounds. The culture medium was removed from the plates after 48 h of culture, and each well was washed once with 200 μL phosphate-buffered saline (PBS, pH = 7.2). The reaction was stopped with the addition of 10 μl of 1 M NaOH, and colour development was assayed at 405 nm using a microplate reader (BIO-RAD 680). The nonenzymatic hydrolysis of the p-NPP (p-nitrophenol phosphate ester) substract was determined for each assay by including wells that did not contain cells as blank wells. Cell survival was expressed as an absorbance (*A*) percentage defined by ($A_{drug\text{-}blank}/A_{control\text{-}blank} \times 100$).

3. Results and discussion

3.1. Characterization of compounds

3.1.1. Properties and structures of the complexes

The complexes are soluble in ethanol, methanol, DMF (N,N-dimethylformamide) and DMSO (dimethyl sulfoxide), insoluble in diethyl ether. They are all air stable. The crystals of the three Cu(II) complex are obtained by evaporating method. The structures of the three complexes are shown in Fig. 1.

3.1.2. Crystal structures of the Cu(II) complexes

The ORTEP representation of the structure of CuL^1, including atom numbering scheme, is shown in Fig. 1(a) and the selected bond lengths and bond angles are listed in Table 2. The coordination of H_2L^1 with Cu(II) ion results in the formation of a five membered (CuONNC) and a six membered (CuNCCCO) chelating rings. Furthermore, there is an ethanol molecule which takes part in coordination (Cu^1–O^3, 1.9465(18) Å) and another ethanol molecule that is non-coordinative. On the contrary, the NO_3^- does not coordinate with Cu(II) ion, and the coordination of Cu^1 with $N^1O^1O^2O^3O^4$ gives a square-pyramidal configuration, and the carbonyl group [C^{12}-O^2, 1.278(3) Å] of benzoyl hydrazine exists as enolization to achieve the charge balance. In addition, in the X-ray structural analysis, one unit cell of the crystal of CuL^1 contains four CuL^1 molecules, but they are not independent crystallographically.

The ORTEP representation of the structure of CuL^2, including atom numbering scheme, is shown in Fig. 1(b) and the selected bond lengths and bond angles are listed in Table 3. The coordination of H_2L^2 with Cu(II) ion results in the formation of a five membered (CuONNC) and a six membered (CuNCCCO) chelating rings. Furthermore, there is two methanol molecules in the Cu(II) crystal structure, one takes part in coordination (Cu^1–O^4, 2.194 Å) and the other is non-coordinative. The nitrate has proved to be a very useful ligand for the construction of coordination complex. There is a nitrate which takes part in coordination with monodentate type in the crystal. Also, there is a free nitrate in the lattice. In addition, in the X-ray structural analysis, one unit cell of the crystal of CuL^2 contains the two CuL^2 molecules, and they are crystallographically symmetrical in the lattice.

The ORTEP representation of the structure of CuL^3, including atom numbering scheme, is shown in Fig. 1(c) and the selected bond lengths and bond angles are listed in Table 4. The coordinated configuration (square-pyramidal) of Cu(II) for ion CuL^3 is similar to CuL^1, where each Cu(II) ion is five-coordinated with two oxygen atoms and one nitrogen atom from H_2L^3 and one oxygen atom of

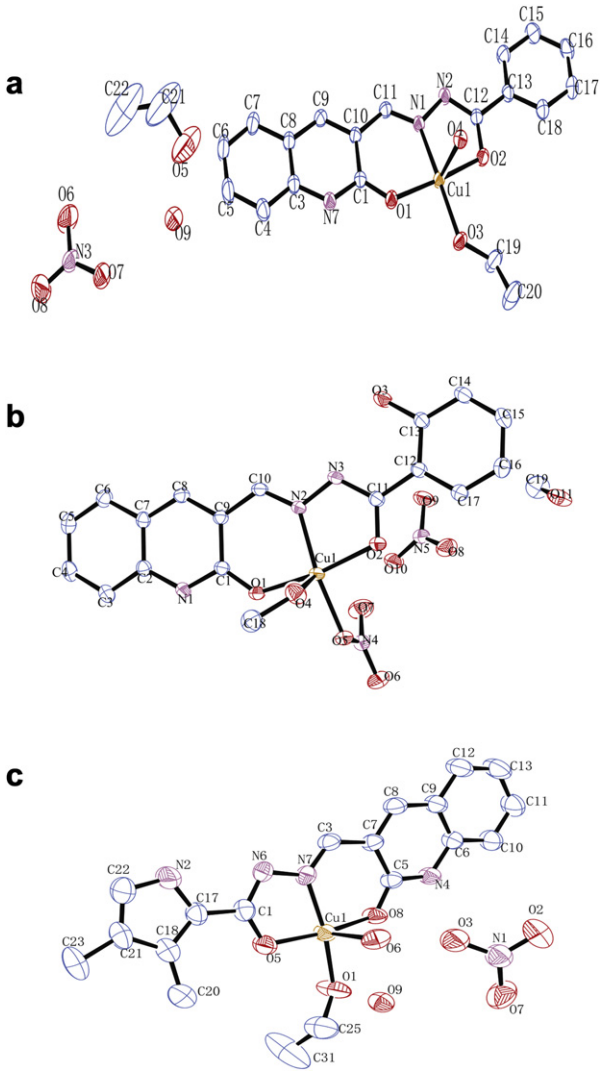

Fig. 1. ORTEP view of (a) (CuL^1), (b) (CuL^2) and (c) (CuL^3) showing the atom numbering of scheme and 30% thermal ellipsoids probability for the non-hydrogen atoms.

H_2O and ethanol molecules. The carbonyl radical [C^1–O^5, 1.290 (4) Å] from 3,4-Dimethylpyrryl-2-carboxylic acid hydrazide also take enolization which is same to that of CuL^1. A free water molecule and nitrate are not coordinated with the Cu(II) ion. Additionally, there are two CuL^3 molecules in one unite of the crystal of CuL^3.

3.2. DNA-binding mode and affinity

3.2.1. Electronic absorption spectrum titration

The binding modes of complexes to DNA are characterized classically through electronic absorption titrations. After the complexes intercalate to the base pair of DNA, the π^* orbital of the intercalated ligands on the complexes could couple of with π orbitals of the base pairs, thus decreasing the π–π^* transition energies. On the other hand, the coupling π^* orbital are partially filled by electrons, thus decreasing the transition probabilities [25]. Therefore, these interactions can result in obvious hypochromism and redshift which were corresponded to what were reported previously [26]. As shown in Fig. 2, the absorption bands of CuL^1, CuL^2 and CuL^3 at 208 nm exhibit hypochromism of about 44.0%, 80.77% and 52.2%, simultaneously, following the hypochromism associated with binding of the two complexes to the DNA helix [27],

Table 2
Selected bond lengths (Å) and angles (°) for the CuL^1.

Bond names	Bond lengths	Bond angles	Angle
Cu1–O2	1.9288(18)	O2–Cu1–N1	81.07(8)
Cu1–N1	1.926(2)	O2–Cu1–O1	172.68(7)
Cu1–O1	1.9276(17)	N1–Cu1–O1	93.10(8)
Cu1–O3	1.9465(18)	O2–Cu1–O3	95.76(8)
Cu1–O4	2.3647(18)	N1–Cu1–O3	170.73(9)
O2–C12	1.278(3)	O1–Cu1–O3	89.31(8)
N1–C11	1.287(3)	O2–Cu1–O4	88.40(7)
N1–N2	1.397(3)	N1–Cu1–O4	96.86(8)
O1–C1	1.271(3)	O1–Cu1–O4	96.73(7)
N7–C1	1.338(3)	O3–Cu1–O4	91.74(8)
N7–C3	1.385(3)	C12–O2–Cu1	110.83(15)
N2–C12	1.325(3)	C11–N1–N2	117.1(2)
O3–C19	1.417(4)	C11–N1–Cu1	128.23(17)
C12–C13	1.486(3)	N2–N1–Cu1	114.68(15)
C11–C10	1.439(3)	C1–O1–Cu1	126.90(17)
C13–C14	1.382(4)	C1–N7–C3	125.1(2)
C13–C18	1.379(4)	C12–N2–N1	108.36(19)
C1–C10	1.448(3)	C19–O3–Cu1	125.40(19)
C10–C9	1.367(3)	O2–C12–N2	124.6(2)
C8–C3	1.400(4)	O2–C12–C13	117.8(2)
C8–C9	1.406(4)	N2–C12–C13	117.2(2)
C8–C7	1.415(4)	N1–C11–C10	123.4(2)
C3–C4	1.393(4)	N1–C11–H11	118.3
C7–C6	1.361(5)	O1–C1–N7	117.3(2)

the absorption of CuL^1, CuL^2 and CuL^3 at 208 nm have 2 nm, 4 nm and 5 nm redshifts, respectively, which are the characteristic of intercalation in the presence of CT-DNA. According to the electronic absorption spectrum, we can deduce initially that the three Cu(II) complexes can bind to DNA by intercalation, but the binding mode need to be proved through more experiments.

3.2.2. Fluorescence spectrum titration

As reported, the fluorescence emission spectrum has been found to be able to distinguish the binding modes of drugs to DNA [28]. The three Cu(II) complexes can emit weak luminescence in Tris–HCl buffer with a max emission wavelength of about 450 nm. The fluorescence titrations with DNA are conducted by keeping the concentrations of complexes constant, and varying the DNA concentrations. Fig. 3 displays the titration curves of the compounds with CT-DNA. The addition of the two Cu(II) complexes leads to the conspicuous increase in the fluorescence emission which clearly indicates that the binding mode of complexes with CT-DNA can be

Table 3
Selected bond lengths (Å) and angles (°) for the CuL^2.

Bond names	Bond lengths	Bond angles	Angle
Cu1–O2	1.9739(18)	O1–Cu1–N2	90.41(7)
Cu1–N2	1.9539(19)	O1–Cu–O2	169.92(7)
Cu1–O1	1.9354(17)	N2–Cu1–O2	80.84
Cu1–O4	2.194(2)	O1–Cu1–O5	93.03(7)
Cu1–O5	1.9752(17)	N2–Cu1–O5	167.35(8)
C1–O1	1.263(3)	O2–Cu1–O5	94.48(7)
C1–N1	1.339(3)	O1–Cu1–O4	92.64(8)
C2–N1	1.390(3)	N2–Cu1–O4	104.30(8)
C10–N2	1.279(3)	O2–Cu1–O4	94.37(8)
C11–N3	1.340(3)	O5–Cu1–O4	87.72(8)
C13–O3	1.350(3)	O1–C1–N1	117.4(2)
C11–O2	1.255(3)	N1–C2–C7	118.2(2)
C11–O3	1.340(3)	O1–C1–C9	125.5(2)
C18–O4	1.425(4)	C3–C2–N1	120.6(2)
C19–O11	1.381(4)	N2–C10–C9	122.5(2)
N2–N3	1.372(3)	N3–C11–C12	120.0(2)
N5–O10	1.227(3)	O3–C13–C14	122.3(2)
N5–O9	1.243(3)	O3–C13–C12	118.2(2)
N5–O8	1.242(3)	N4–O5–Cu1	111.17(15)

Table 4
Selected bond lengths (Å) and angles (°) for the CuL^3.

Bond names	Bond lengths	Bond angles	Angle
Cu1–O1	1.951(2)	O5–Cu1–O8	167.75(9)
Cu1–O5	1.916(2)	O5–Cu1–N7	81.76(9)
Cu1–O6	2.275(2)	O8–Cu1–N7	93.18(9)
Cu1–N7	1.940(2)	O5–Cu1–O1	94.43(10)
Cu1–O8	1.929(2)	O8–Cu1–O1	88.58(9)
N1–O2	1.209(4)	N7–Cu1–O1	169.42(11)
N1–O7	1.243(4)	O5–Cu1–O6	96.78(10)
N1–O3	1.255(4)	O8–Cu1–O6	94.74(9)
N6–N7	1.385(3)	N7–Cu1–O6	94.61(9)
C1–O5	1.290(4)	O1–Cu1–O6	95.64(11)
C1–N6	1.332(4)	O2–N1–O7	120.9(3)
C5–O8	1.267(3)	C5–N4–C6	125.8(2)
C5–N4	1.346(3)	C1–N6–N7	109.4(2)
C22–N2	1.352(4)	C3–N7–Cu1	127.26(19)
C25–O1	1.452(4)	N6–N7–Cu1	113.87(17)
C3–C7	1.450(4)	C25–O1–Cu1	126.0(2)
C6–N4	1.384(3)	C5–O8–Cu1	125.93(17)
C6–C10	1.389(4)	C1–O5–Cu1	110.91(18)
C9–C12	1.423(4)	O8–C5–N4	117.2(2)

intercalation. Because the enhancement of fluorescence intensity implied that these compounds can insert between DNA base pair, as a result, these compounds are protected from solvent water molecules by the hydrophobic environment inside the DNA helix [29]. The microenvironment of fluorophores residue change accordingly and the accessibility of solvent water molecules to these compounds is reduced. And that an enhanced fluorescence is believed to be one of the criteria for intercalative binding [30,31]. According to the Scatchard equation, a plot of r/C_f versus r gives the intrinsic binding constants of the compounds. The results imply that all the compounds can insert between DNA base pairs and CuL^3 ($K_b = 3.3 \times 10^6\ M^{-1}$) can interact with DNA more strongly than CuL^1 ($K_b = 1.27 \times 10^6\ M^{-1}$) and CuL^2 ($K_b = 2.76 \times 10^6\ M^{-1}$). However, the DNA-drugs binding modes and binding affinity need to be proved further by viscosity studies and EB–DNA displacement experiment.

3.2.3. Viscosity measurements

Measurements of DNA viscosity that is sensitive to DNA length change are regarded as the least ambiguous and the most critical tests of binding in solution in the absence of crystallographic structural data [32]. An intercalative mode drug to DNA will lead to obvious increase of DNA viscosity [33]. Fig. 4 shows that the three Cu(II) complexes cause a remarkable increase of viscosity and the increasing degree of relative viscosity, which may be depend on its affinity to DNA, follows the order of $CuL^3 > CuL^2 > CuL^1$. The observed phenomenon is consistent with that of a classical intercalation and can be caused by different terminal ligands.

3.2.4. DNA–EB competitive experiment

Ethidium bromide (EB) is one of the most sensitive fluorescent probes which can bind to DNA through intercalation [34,35]. Competitive binding to DNA of the drugs with EB could provide rich information with regard to the DNA-binding affinity. As shown in Fig. 5, the fluorescence intensity decrease obviously with the increasing concentration of the three Cu(II) complexes. The K_q values for Cu(II) complexes are $6.75 \times 10^4\ M^{-1}$ (CuL^1), $1.81 \times 10^5\ M^{-1}$ (CuL^2) and $2.48 \times 10^5\ M^{-1}$ (CuL^3), respectively. The quenching plots illustrate that the quenching of EB bound to DNA by the compounds are in good agreement with the linear Stern–Volmer equation and the binding ability of three compounds follows the order $CuL^3 > CuL^2 > CuL^1$ which are in agreement with the fluorescence and viscosity measurements. Furthermore, such quenching constants of the Cu(II) complexes suggest that the interaction of all the compounds with DNA should be of intercalation [36].

3.3. Cytotoxic activity

The cytotoxicity assays of ligands and Cu(II) complexes against two kinds of tumor cells [human leukemia HL-60 and uterine cervix carcinoma cell (Hela)] are shown in Fig. 6(a) and (b). The biological assays of the ligands and Cu(II) complexes show Cu(II) complexes exhibit more significant activities than corresponding ligands against HL-60 and Hela cells. For HeLa cell line CuL^3 ($IC50 = 38\ \mu M$) demonstrated a much higher inhibitory effect than CuL^2 ($IC50 = 43\ \mu M$), CuL^1 ($IC50 > 160\ \mu M$) shows nearly no activity. Moreover, the inhibitory effects of compounds ($IC50CuL^1 = 19\ \mu M$, $IC50CuL^2 = 18\ \mu M$, $IC50CuL^3 = 8\ \mu M$) for HL-60 cell follow the order $CuL^3 > CuL^2 > CuL^1$. The CuL^3 whose IC50 is 8 μM is especially most active. The cytotoxic activity studies in vitro indicate that the three Cu(II) complexes have rather activities than corresponding ligands against the two tumor cells, the three Cu(II) complexes which possess better cytotoxic activities than ligands may be attributed to the extended planar structure induced by the $p-\pi^*$ conjugation resulting from the chelating of the metal ion with ligand. In addition, the inhibitory rates of CuL^3 against the two tumor cells are higher than CuL^1 and CuL^2, which can be caused by the 3,4-dimethylpyrryl heterocycle from CuL^3.

4. Conclusion

In this paper, three new 2-oxo-quinoline-3-carbaldehyde Schiff-bases ligands and their Cu(II) complexes are synthesized and

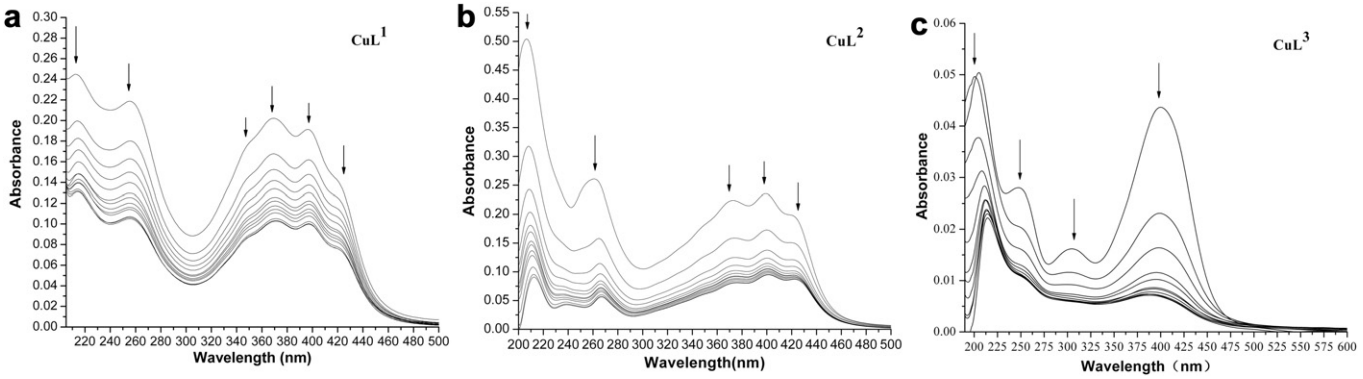

Fig. 2. Absorption spectra of CuL^1 (a), CuL^2 (b) and CuL^3 (c) (10 μM) in the absence and presence of increasing amounts of CT-DNA (0, 2.5, 5, 7.5, 10, 12.5, 15, 17.5, 20, 22.5, 25, 27.5, 30 μM; subsequent spectra). Arrows show the absorbance changes upon increasing DNA concentration.

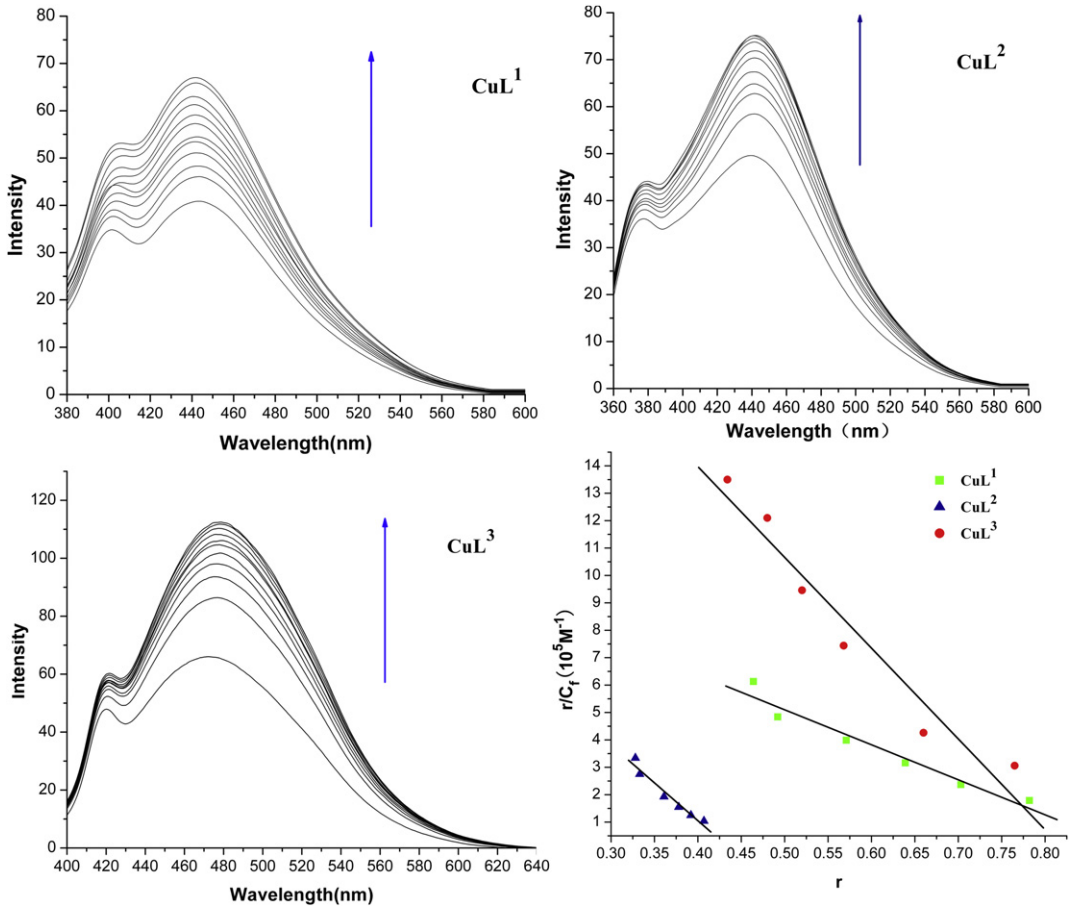

Fig. 3. Emission enhancement spectra of compounds [CuL^1, CuL^2 and CuL^3 (10 μM)] in the absence and presence of increasing amounts of CT-DNA (2.5, 5, 7.5, 10, 12.5, 15, 17.5, 20, 22.5, 25, 27.5, 30 μM); $\lambda_{ex} = 370$ nm, $\lambda_{em} = 450$ nm. Arrows show the emission intensity changes of upon the increasing CT-DNA concentration. Inset: Scatchard plot of the fluorescence titration data of compounds, $K_b = 1.27 \times 10^6\ M^{-1}$ (CuL^1). $K_b = 2.76 \times 10^6\ M^{-1}$ (CuL^2). $K_b = 3.30 \times 10^6\ M^{-1}$ (CuL^3).

characterized. And that the X-ray diffraction shows the three Cu(II) complexes exhibit similar coordinative modes. In addition, the binding modes of CT-DNA to the Cu(II) complexes are also studied. The photophysical and viscosity measurements indicate that the three Cu(II) complexes can interact with CT-DNA through intercalative binding modes, respectively. The cytotoxicities of the three Cu(II) complexes are tested in vitro and the biological assays suggest the Cu(II) complexes exhibit higher activity than corresponding ligands against HeLa and HL-60 cells, which can be attributed to the interaction between Cu(II) ion and ligands. Moreover, the most active compound is CuL^3 which may be explained as resulting from a difference in the terminal functional group (3,4-dimethylpyrryl heterocycle) relative to CuL^1 and CuL^2. The finding are significant for us to explore the DNA-binding studies and cytotoxic activities on the Cu(II) Schiff-bases complexes of quinolone derivates.

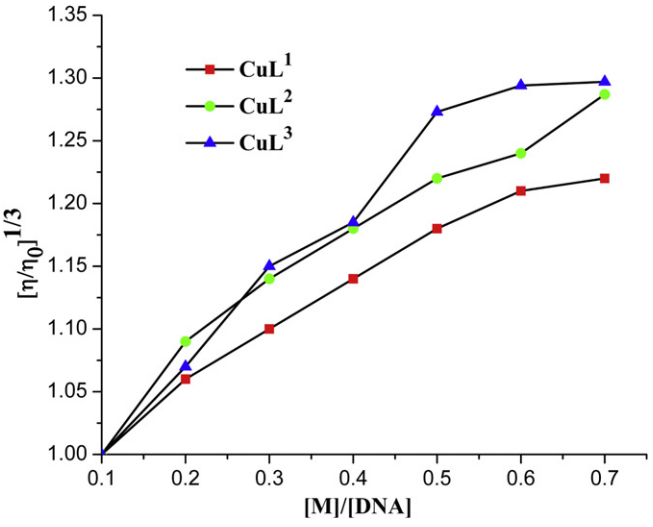

Fig. 4. Effect of increasing amounts of CuL^1, CuL^2 and CuL^3 on the relative viscosity of CT-DNA at 25.0 ± 0.1 °C, [DNA] = 5.0 μM.

5. Experimental protocols

5.1. DNA-binding study methods

5.1.1. Electronic spectral titration

Absorption titration experiment was performed by maintaining the three Cu(II) complexes concentration constant (10 μM) and gradually increasing the concentration of CT-DNA. The compounds were dissolved in a mixed solvent of 1% CH_3OH and 99% Tris–HCl buffer. The reference solution was the corresponding Tris–HCl buffer solution. While measuring the absorption spectra, equal amount of CT-DNA was added to both compound solution and the reference solution to eliminate the absorbance of CT-DNA itself. The sample solution was scanned in the range 200–500 nm.

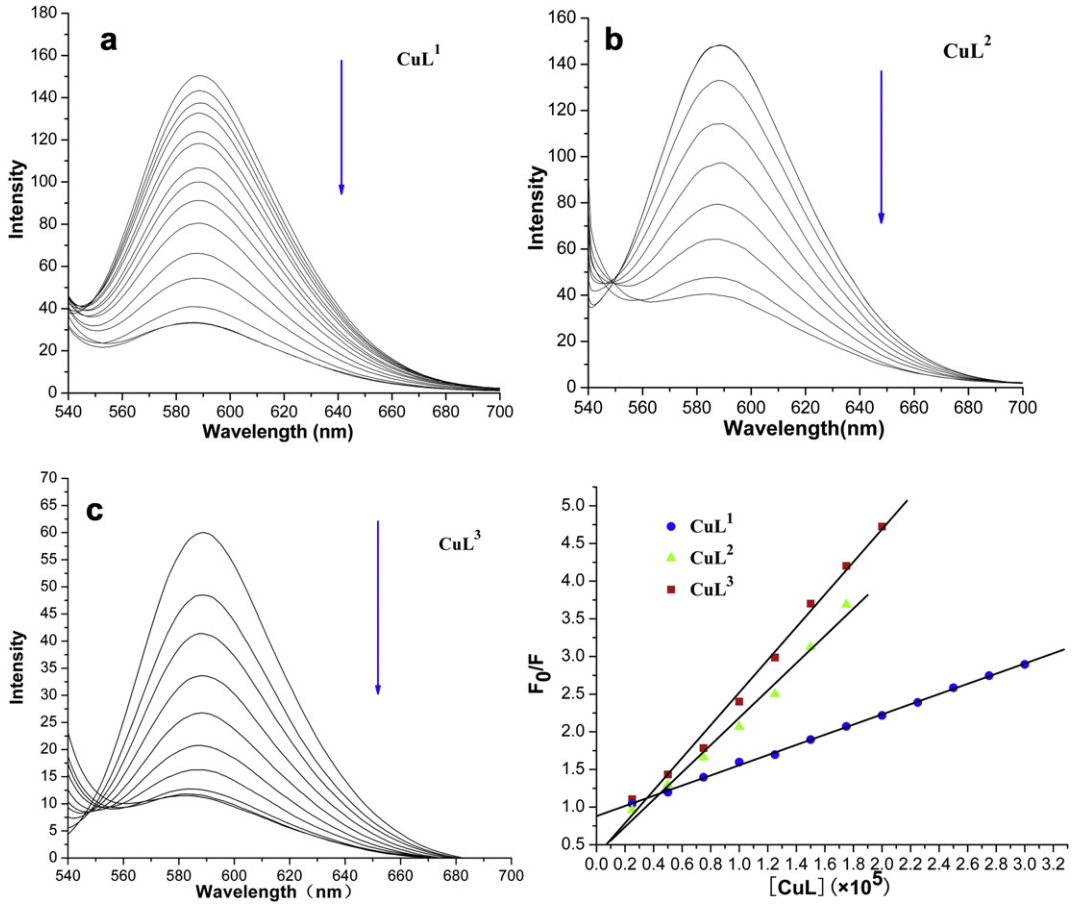

Fig. 5. Emission spectra of DNA–EB system (10 μM DNA and 0.33 μM EB), $\lambda_{ex} = 521$ nm, $\lambda_{em} = 540–700$ nm, in the presence of (0, 2.5, 5, 7.5, 10, 12.5, 15, 17.5, 20, 22.5, 25, 27.5, and 30 μM) CuL^1 (a), CuL^2 (b) and CuL^3 (c). Arrows show the emission intensity changes upon increasing compounds concentration. Stern–Volmer plots of the fluorescence titration of CuL^1 (a), CuL^2 (b) and CuL^2 (c). Quenching constant $K_q = 6.75 \times 10^4\ M^{-1}$ (CuL^1), $K_q = 1.81 \times 10^5\ M^{-1}$ (CuL^2), $K_q = 2.48 \times 10^5\ M^{-1}$ (CuL^3).

5.1.2. Fluorescence spectral titration

To investigate the binding modes and compare further the affinity of the compounds bound to CT-DNA, the fluorescence titration spectrum was studied A fixed amount of the compound (10 μM) was titrated with increasing amounts of CT-DNA. The samples were excited at 370 nm and the total fluorescence emission intensity was monitored at 450 nm for the Cu(II) complexes. *K* values were determined using the following equations [32].

$$r/C_f = K_b(1 - nr)$$

where $r = C_b/[DNA]$, $C_f = C_t[(F - F_0)/(F_{max} - F_0)]$, C_b and C_t is the concentration of free compound and the total compound, respectively. *F* is the observed fluorescence emission intensity at a given DNA concentration, F_0 is the intensity in the absence of DNA, and F_{max} is the fluorescence intensity of the totally bound compound. Binding data were casted into the form of a Scatchard plot of r/C_f

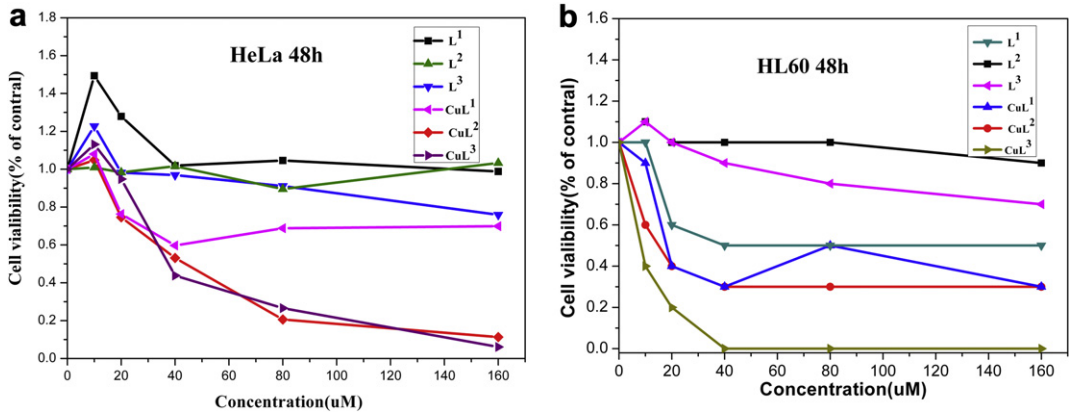

Fig. 6. (a) Cytotoxic activity of compounds against HeLa. (b) Cytotoxic activity of compounds against HL-60.

versus *r*. All experiments were conducted at 20 °C in a buffer containing 5 mM Tris–HCl (pH = 7.2) and 50 mM NaCl.

5.1.3. Viscosity measurement experiment

The viscosity titrations were conducted on an Ubbelohde viscometer in a thermostatic water bath maintained at 298 (±0.1) K. The DNA concentration was kept constant (5 μM) and gradually increased the concentration of tested compound (0.5–3.5 μM). The time of the solution's flowing through the capillary was determined to the nearest 0.02 s by a stop-watch with the viscometer. Each sample was measured three times and an average flow was calculated at last. Data were presented as $(\eta/\eta_0)^{1/3}$ versus the ratio of the concentration of the compound to CT-DNA, where η was the viscosity of CT-DNA in the presence of the compound and η_0 was the viscosity of CT-DNA alone. Viscosity values were calculated from the observed flow time of CT-DNA containing solutions corrected from the flow time of buffer alone (t_0), $\eta = t - t_0$.

5.1.4. EB–DNA competition experiment

EB–DNA experiments were conducted by adding the compounds solution to the Tris–HCl buffer of EB–DNA. The change of fluorescence intensity was recorded. The excitation and the emission wavelength were 521 nm and 587 nm, respectively. According to the classical Stern–Volmer equation:

$$F_0/F = K_q[Q] + 1$$

where F_0 is the emission intensity in the absence of quencher, F is the emission intensity in the presence of quencher, K_q is the quenching constant, and [Q] is the quencher concentration. The plots can be used to characterize the quenching as being predominantly dynamic or static. Plots of F_0/F versus [Q] appear to be linear.

5.2. Preparation and characterization of compounds

As shown in Scheme 1, 3,4-dimethylpyrryl-2-carboxylic acid hydrazine **2** was prepared easily by refluxing 3,4-dimethyl-2-ethoxycarbonyl-pyrrole **1** (0.5 g, 3 mmol) with stirring in an ethanol solution (30 mL) containing hydrazine hydrate (80%, 0.375 g, 6 mmol). After cooling to room temperature, a white precipitation separated out. The precipitation was filtrated under decompression and washed with ethanol. Recrystallization from CH_3OH/H_2O (V:V = 1:2) gave the white product in 70% yield. m.p.:218–220 °C. ^{1}H-NMR (DMSO-d_6 ppm): δ 10.62 (1H, s, pyrrole –NH), δ 8.51 (1H, s, –NH–C=O), δ 6.59 (1H, d, pyrrole –CH), δ 4.27 (2H, s, $-NH_2$), δ 2.13 (3H, s, $-CH_3$), δ 1.90 (3H, s, $-CH_3$). ^{13}C-NMR (DMSO-d_6 ppm): δ:162.34, 121.24, 121.00, 118.19, 117.98, 10.10, 9.79. The ^{13}C-NMR spectrum is shown in Fig. S1 (Supplementary information).

2-Oxo-quinoline-3-carbaldehyde ***5***. Yield, 85%. Colour, yellow. m.p.:303–305 °C. ^{1}H-NMR (DMSO-d_6 ppm): δ 12.24 (1H, s, $-N^1H$), δ 10.24 (1H, s, –CHO), δ 8.51 (1H, s, $-C^4-H$), δ 7.92 (1H, d, $-C^5-H$), δ 7.66 (1H, t, $-C^6-H$), δ 7.25 (1H, t, $-C^7-H$), δ 7.35 (1H, d, $-C^8-H$).

2-Oxo-quinoline-3-carbaldehyde-benzoyl hydrazone (H_2L^1) **6a** was synthesized by the following method (Scheme 1). An ethanol solution (10 mL) containing benzoyl hydrazine (0.48 g, 3.5 mmol) was added to another ethanol solution (10 mL) containing 2-oxo-quinoline-3-carbaldehyde **5** (0.6 g, 3.5 mmol). The mixture was refluxed for twelve hours with stirring and a white precipitation separated out. The precipitation was filtrated under decompression and washed with ethanol. Recrystallization from DMF/H_2O (V:V = 1:1) gave the yellow ligand H_2L^1, which was dried under vacuum. Yield, 85%. m.p.:307–309 °C. ^{1}H-NMR (DMSO-d_6 ppm): δ 12.055 (1H, s, $-N^1-H$), δ 12.025 (1H, s, $-N^{3'}-H$), δ 8.723 (1H, s, –CH=N), δ 8.487 (1H, s, $-C^4-H$), δ 7.932–7.957 (2H, s, $-C^{6',10'}-H$), δ 7.861–7.889 (1H, m, $-C^{7'}-H$), δ 7.512–7.633 (4H, m, $-C^{5,6,7,8}-H$), δ 7.330–7.357 (1H, m, $-C^{9'}-H$), δ 7.199–7.250 (1H, m, $-C^{8'}-H$).

2-Oxo-quinoline-3-carbaldehyde-2-hydroxybenzoyl hydrazone (H_2L^2) **6b** and 2-oxo-quinoline-3-carbaldehyde-3,4-dimethyl-pyrryl-2-carboxylic acid hydrazone (H_2L^3) **6c** were synthesized according to the same procedure as the synthesis method of ligand H_2L^1. H_2L^2, Yield, 76%. Colour, yellow. m.p.:314–316 °C. ^{1}H-NMR (DMSO-d_6, ppm): δ 12.043 (2H, s, $-N^1-H$, $-N^{3'}-H$), δ 11.875 (1H, s, –OH), δ 8.715 (1H, s, –CH=N), δ 8.496 (1H, s, $-C^4-H$), δ 7.861–7.922 (2H, m, $-C^{6',9'}-H$), δ 7.527–7.578 (1H, m, $-C^5-H$), δ 7.424–7.475 (1H, m, $-C^7-H$), δ 7.334–7.361 (1H, m, $-C^8-H$), δ 7.201–7.252 (1H, m, $-C^6-H$), δ 6.928–6.986 (1H, m, $-C^{7',8'}-H$). H_2L^3, Yield, 80%. Colour, khaki. m.p.:317–319 °C. ^{1}H-NMR (DMSO-d_6, ppm): δ 12.171 (1H, s, $-N^1-H$,), δ 11.242 (1H, s, $-N^{3'}-H$), δ 8.352 (1H, s, –CH=N), δ 8.302 (1H, s, $-C^4-H$), δ 7.800–7.802 (1H, m, $-N^5-H$), δ 7.532–7.574 (1H, m, $-N^7-H$), δ 7.333–7.354 (1H, m, $-N^8-H$), δ 7.217–7.254 (1H, m, $-N^6-H$), δ 6.750–6.756 (1H, m, $-N^{6'}-H$), δ 3.337 (1H, s, $-N^{7'}-H$), δ 2.252 (3H, s, $-C^{11'}-H$), δ 1.970 (3H, s, $C^{9'}-H$).

5.3. Preparation of Cu(II) complexes

The ligand H_2L^1 (0.2 mmol, 0.0582 g) and Cu(II) nitrate (0.2 mmol, 0.0483 g) were added to ethanol (10 mL). After 5 min, the mixtures were filtered to remove any insoluble residues and then were stirred for 10 h under reflux. A green precipitation (yield:85%) of the Cu(II) complex was separated from the solution by suction filtration, purified by washing several times with Ethanol and dried for 24 h under vacuum. The Cu(II) complex was characterized by X-ray single crystal diffraction.

The Cu(II) complex of H_2L^2 and H_2L^3 was prepared by the same method. The ligand H_2L^2 (0.2 mmol, 0.0614 g) and Cu(II) nitrate (0.2 mmol, 0.0483 g) were added to methanol (10 mL). After 5 min, the mixtures were filtered to remove any insoluble residues and then were stirred for 10 h under reflux. A green precipitation (yield:80%) of the Cu(II) complex was separated from the solution by suction filtration, purified by washing several times with methanol and dried for 24 h under vacuum. The Cu(II) complex was characterized by X-ray single crystal diffraction. The ligand H_2L^3 (0.2 mmol, 0.061 g) and Cu(II) nitrate (0.2 mmol, 0.0483 g) were added to ethanol (10 mL). After 5 min, the mixtures were filtered to remove any insoluble residues and then were stirred for 10 h under reflux. A brown precipitation (yield:75%) of the Cu(II) complex was separated from the solution by suction filtration, purified by washing several times with ethanol and dried for 24 h under vacuum. The Cu(II) complex was characterized by X-ray single crystal diffraction.

Acknowledgements

This work is supported by the National Natural Science Foundation of China (20975046).

Appendix. Supplementary information

Crystallographic data for the structural analysis have been deposited with the Cambridge Crystallographic Data Centre, CCDC (737811, 746589, 763151). Copy of this information may be obtained free of charge from the Director, CCDC, 12 Union Road, Cambridge, CB2 1EZ, UK (fax: +44 1223 336033; e-mail: deposit@ccdc.cam.ac.uk or http://www.ccdc.cam.ac.uk/deposit).

Supplementary data associated with this article can be found in the online version, at doi:10.1016/j.ejmech.2010.08.060.

References

[1] K.E. Erkkila, D.T. Odom, J.K. Barton, Chem. Rev. 99 (1999) 2777–2795.
[2] J.K. Barton, A.L. Raphael, J. Am. Chem. Soc. 106 (1984) 2466–2468.
[3] A. Chouai, S.E. Wicke, C. Turro, J. Bacsa, K.R. Dunbar, D. Wang, R.P. Thummel, Inorg. Chem. 44 (2005) 5996–6003.
[4] J. Hooda, D. Bednarski, L. Irish, S.M. Firestine, Bioorg. Med. Chem. 14 (2006) 1902–1909.
[5] F. Liang, P. Wang, X. Zhou, T. Li, Z.Y. Li, H.K. Lin, D.Z. Gao, C.Y. Zheng, C.T. Wu, Bioorg. Med. Chem. Lett. 14 (2004) 1901–1904.
[6] J.M. Kelly, A.B. Tossi, D.J. McConnel, C. O'Huigin, Nucleic Acids Res. 13 (1985) 6017–6034.
[7] G.M. Zhang, S.M. Shuang, C. Dong, D.S. Liu, M.F. Choi, J. Photochem. Photobiol. B 74 (2004) 127–134.
[8] S. Sharma, S.K. Singh, M. Chandra, D.S. Pandey, J. Inorg. Biochem. 99 (2005) 458–466.
[9] S. Padhye, G.B. Kauffman, Coord. Chem. Rev. 63 (1985) 127–160.
[10] L. Wang, Y. Zhu, Z. Yang, J. Wu, Q. Wang, Polyhedron 10 (1991) 2477–2481.
[11] I.-ul-H. Bhat, S. Tabassum, Spectrochim. Acta Part A 72 (2009) 1026–1033.
[12] V. Uma, M. Kanthimathi, T. Weyhermuller, B.U. Nair, J. Inorg. Biochem. 99 (2005) 2299–2307.
[13] P.-D. Duh, S.-C. Wu, L.-W. Chang, H.-L. Chu, W.-J. Yen, B.-S. Wang, Food Chem. 114 (2009) 87–92.
[14] H. Paritala, S.M. Firestine, Bioorg. Med. Chem. Lett. 19 (2009) 1584–1587.
[15] M. Andaloussi, E. Moreau, N. Masurier, J. Lacroix, R.C. Gaudreault, J.M. Chezal, A.E. Laghdach, D. Canitrot, E. Debiton, J.C. Teulade, O. Chavignon, Eur. J. Med. Chem. 43 (2008) 2505–2517.
[16] J. DeRuiter, A.N. Brubaker, W.L. Whitmer, J.L. Stein, J. Med. Chem. 29 (1986) 2024–2028.
[17] P. Hewawasam, W.H. Fan, J. Knipe, S.L. Moon, C.G. Boissard, V.K. Gribkoff, J.E. Starett, Bioorg. Med. Chem. Lett. 12 (2002) 1779–1783.
[18] Z.C. Liu, B.D. Wang, Z.Y. Yang, Y. Li, D.D. Qin, T.R. Li, Eur. J. Med. Chem. 44 (2009) 4477–4484.
[19] M.K. Rauf, Imtiaz-ud-Din, A. Badshah, M. Gielen, M. Ebihara, Dick de Vos, S. Ahmed, J. Inorg. Biochem. 103 (2009) 1135–1144.
[20] M.P. Sathisha, Ullas N. Shetti, V.K. Revankar, K.S.R. Pai, Eur. J. Med. Chem. 43 (2008) 2338–2346.
[21] M. Porchia, F. Benetollo, F. Refosco, F. Tisato, C. Marzano, V. Gandin, J. Inorg. Biochem. 103 (2009) 1644–1651.
[22] M.K. Singh, A. Chandra, B. Singh, R.M. Singh, Tetrahedron Lett. 48 (2007) 5987–5990.
[23] A. Helms, D. Heiler, G. Mclendon, J. Am. Chem. Soc. 114 (1992) 6227–6238.
[24] Q. Wang, Y. Wang, Z.Y. Yang, Chem. Pharm. Bull. 56 (2008) 1018–1021.
[25] C.Y. Zhong, J. Zhao, Y.B. Wu, C.X. Yin, P. Yang, J. Inorg. Biochem. 101 (2007) 10–18.
[26] M.A. Pyle, P.J. Rehmann, R. Meshoyrer, J.N. Kumar, J.N. Turro, K.J. Barton, J. Am. Chem. Soc. 111 (1989) 3053–3063.
[27] C.V. Kumar, H.E. Asuncion, J. Am. Chem. Soc. 115 (1993) 8547–8553.
[28] H. Xu, L. Yi, P. Zhang, F. Du, B.R. Zhou, J. Wu, J.H. Liu, Z.G. Liu, L.N. Ji, J. Biol. Inorg. Chem. 10 (2005) 529–538.
[29] A.E. Friedman, J.C. Chambron, J.P. Sauvage, N.J. Turro, J.K. Barton, J. Am. Chem. Soc. 112 (1990) 4960–4962.
[30] B.D. Wang, Z.Y. Yang, T.R. Li, Bioorg. Med. Chem. 14 (2006) 6012–6021.
[31] Z.Y. Yang, B.D. Wang, Y.H. Li, J. Org. Met. Chem. 691 (2006) 4159–4166.
[32] S. Satyanarayana, J.C. Dabrowiak, J.B. Chaires, Biochemistry 31 (1992) 9319–9324.
[33] B.Y. Wu, L.H. Gao, Z.M. Duan, K.Z. Wang, J. Inorg. Biochem. 99 (2005) 1685–1691.
[34] F.J. Meyer-Almes, D. Porschke, Biochemistry 32 (1993) 4246–4253.
[35] G.M. Howe, K.C. Wu, W.R. Bauer, Biochemistry 19 (1976) 339–347.
[36] B.D. Wang, Z.Y. Yang, Q. Wang, T.K. Cai, P. Crewdson, Bioorg. Med. Chem. 14 (2006) 1880–1888.